Biophysical Journal, Volume *114*

Supplemental Information

Tissue-Specific Optical Mapping Models of Swine Atria Informed by Optical Coherence Tomography

Theresa H. Lye, Kevin P. Vincent, Andrew D. McCulloch, and Christine P. Hendon

1. Extraction of Tissue Geometry

The image processing steps for surface detection in each dataset are described in further detail below. If errors in the surface detection remained after processing, errors were manually removed or filtering parameters further adjusted within areas of error until a smooth detected tissue corresponding to the imaged tissue surface was obtained. Additionally, for the ablated tissue data, small tissue regions were missing from the OCT images due to the upper tissue surface extending past the upper image field of view in certain B-scans or imperfect alignment of adjacent volumetric data during imaging. Two-dimensional interpolation in MATLAB was used to fill these gaps.

Left Atrium-1 Dataset

To detect the upper (epicardial) surface, a 10 x 10 median filter was applied to smooth speckle noise, before the maximum magnitude of the gradient in the axial direction was detected.

To detect the lower (endocardial) surface, the upper tissue surface was first cropped from the image volume. A 20 x 20 median filter and morphological opening with a disk-shaped structuring element of radius 15 were applied to smooth noise. The image was then thresholded, and morphological closing on the binary image was applied with a disk-shaped structuring element of radius 15 to close gaps in the detected surface. The minimum magnitude of the gradient in the axial dimension was detected.

Left Atrium-2 Dataset

The dataset was downsampled by 3. To smooth speckle noise, a 10 x 10 median filter was applied. The maximum of the gradient magnitude in the axial direction was detected. A 15 x 15 median filter was applied to the detected surface to smooth remaining errors.

Non-transmural Lesion Dataset

A 20 x 20 median filter was applied to smooth speckle noise, and morphological opening with a 30 x 50 rectangular structuring element was applied to minimize vertical streak-like saturation artifacts. The gradient magnitude was computed.

The background signal of the OCT image and blank regions induced by stitching created areas of high gradient magnitude that interfered with the detection of the tissue surface. These areas were removed after calculation of the gradient magnitude by the following steps. First, a 10 x 10 average filter to the original image was applied and the image was thresholded. A dilation of the resulting binary image, with a disk-shaped structuring element of radius 20, was applied to create a binary mask that was zero over the erroneous boundaries. The gradient magnitude matrix was multiplied by this binary mask.

Afterwards, the gradient magnitude was thresholded and detected. The detected surface from each B-scan was median filtered with a kernel size of 15 to smooth the resulting surface.

Transmural Lesion Dataset

The dataset was downsampled by 3. A 5 x 5 median filter was applied. The maximum axial gradient magnitude was detected after removal of erroneous areas of high gradient magnitude in the axial direction caused by stitching, with an equivalent procedure as described above for the non-transmural lesion dataset. The detected surface was median filtered with a 15 x 15 kernel size.

2. Extraction of Ablation Lesion Region

To detect the birefringence artifact, a region of interest up to 50 pixels below the tissue surface was first defined. Within this region, the image was then filtered by a 50 x 50 Laplacian of Gaussian (LoG) filter with a standard deviation of 1. The maximum was taken from each A-line within the LoG filtered image and the 1D vector of maximum gradient values was median filtered by 20 to smooth the extracted trend. Finally, the maximum gradient values were thresholded to separate regions based on whether the birefringence artifact was present or not. This enabled the detection of the boundary of the lesion within each B-scan based on the birefringence artifact.

3. Mesh Generation for Light Scattering Simulation

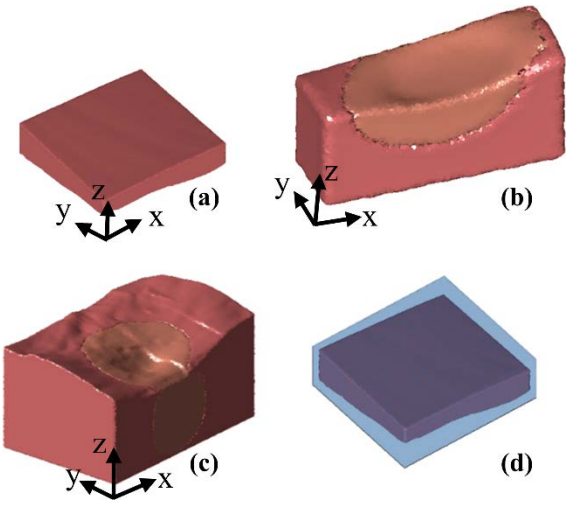

Figure S1. Tetrahedral models for light propagation simulation, generated from OCT data of atrial tissues. **(a)** Left atrium-1 model. **(b)** Non-transmural lesion model. **(c)** Transmural lesion model. **(d)** Left atrium-1 model with surrounding perfusate region.